Miner Deposita (2010) 45:313–321
DOI 10.1007/s00126-010-0277-8

LETTER

The Tropezón Cu–Mo–(Au) deposit, Northern Chile: the missing link between IOCG and porphyry copper systems?

Fernando Tornos · Francisco Velasco · Fernando Barra · Diego Morata

Received: 21 July 2009 / Accepted: 12 January 2010 / Published online: 23 February 2010

Introduction

Despite having been described as an independent style of mineralization sharing common geological and geochemical features (Hitzman et al. 1992; Williams et al. 2005), the nature and origin of iron oxide–copper–gold (IOCG) mineralization is a matter of debate. While some authors postulate a link with basinal brines (Barton and Johnson 1996), others associate IOCG mineralization with magmatic–hydrothermal activity (e.g., Badham 1978; Pollard 2000; Marschik and Fontboté 2001; Sillitoe 2003; Mark et al. 2004).

Editorial handling: B. Lehmann

F. Tornos (✉)
Instituto Geológico y Minero de España,
Azafranal 48,
37001 Salamanca, Spain
e-mail: f.tornos@igme.es

F. Velasco
Dpto. Mineralogía y Petrología, Facultad de Ciencia y Tecnología,
Universidad del País Vasco,
48080 Bilbao, Spain

F. Barra
Department of Geosciences, The University of Arizona,
1040 East Fourth Street,
Tucson, AZ 85721, USA

F. Barra
Instituto de Geología Ecónomica Aplicada,
Universidad de Concepción,
Concepción, Chile

D. Morata
Dpto. Geología, Universidad de Chile,
Plaza Ercilla 803,
Santiago, Chile

The Coastal Cordillera of northern Chile and Peru hosts several IOCG deposits of Late Jurassic–Early Cretaceous age aligned in a 1,000-km-long belt parallel to the Pacific coast. They are usually hosted by sub-aerial andesites or broadly contemporaneous gabbro to granodiorite intrusions formed during the early stages of the Andean magmatic arc (Sillitoe 2003).

The predominant style of IOCG mineralization consists of hematite-rich veins, mantos, and breccia bodies with lesser amounts of chalcopyrite, pyrite, and bornite; mineralization is related to a hydrothermal assemblage with variable proportions of K-feldspar, chlorite, sericite, epidote, carbonates, quartz, actinolite, and scapolite. The largest deposits of this hematite-rich type in Chile are Mantoverde (140 Mt @ 0.63% Cu; Benavides et al. 2007) and Mina Carmen de Cobre (71 Mt @ 0.65% Cu; Herrera et al. 2008). The magnetite-rich variant occurs as veins and replacements with minor chalcopyrite and is characterized by an alteration assemblage of actinolite, biotite, K-feldspar, and quartz. The most significant deposit of this type is Candelaria (470 Mt @ 0.95% Cu; Marschik and Sollner 2006). The IOCG mineralization in the Coastal Cordillera of Chile coexists with large magnetite–apatite ore bodies (>100 Mt) of broadly equivalent age, such as El Romeral or Algarrobo (Fig. 1).

Recent models propose that the IOCG deposit types represent a vertical continuum ranging from deep, magnetite-dominated Cu–Au mineralization to hematite-bearing Cu ore at shallow levels, all associated with geochemically primitive diorite intrusions (Sillitoe 2003). However, so far there has been no detailed description of this proposed genetic connection with igneous rocks. Presumed relationships are based on the broad coincidence in ages, crosscutting relationships and the fact that structures hosting the IOCG mineralization also include intrusive rocks (Sillitoe 2003).

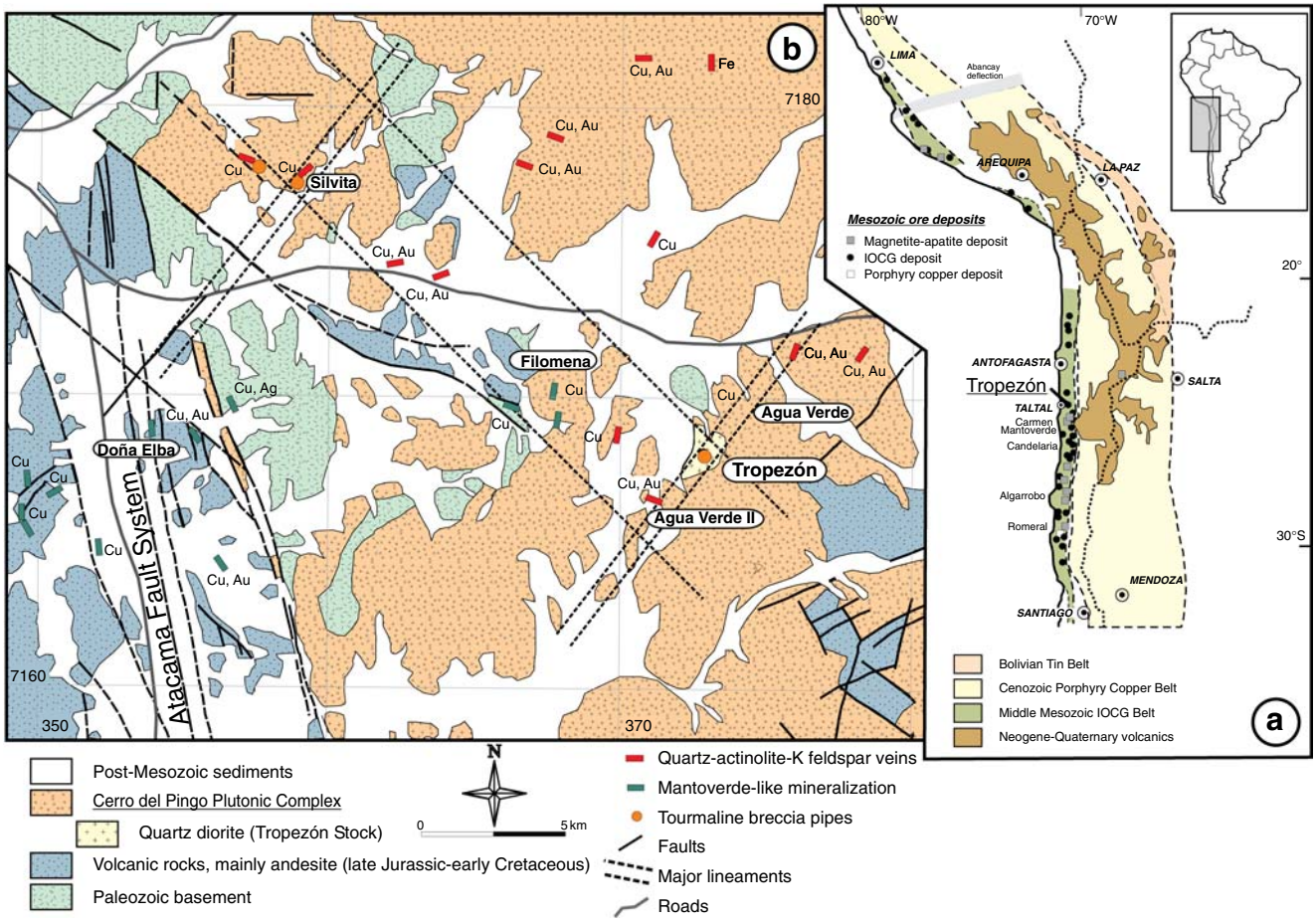

Fig. 1 **a** Geologic map of central and northern Chile showing the location of the late Jurassic–early Cretaceous magmatic arc and related ore deposits. For comparison, other magmatic and ore deposit belts of the Andes are shown. Compiled from Dallmeyer et al. (1996), Lehmann et al. (2000), Marschik and Fontbote (2001), Grocott and Taylor (2002), and Sillitoe (2003). **b** Geology of the study area with the location of the more significant ore prospects, most of IOCG type. The Mantoverde-like prospects include veins and replacements with hematite, K-feldspar, sericite, chlorite, and calcite. Based on Ulriksen (1979) and Naranjo and Puig (1984). UTM Grid

Here we describe an intrusion-related Cu–(Mo–Au)-rich IOCG deposit located at the core of a hydrothermal system that includes both magnetite- and hematite-rich mineralization. We provide evidence that at least some IOCG systems are magmatic in origin and formed by broadly similar processes than porphyry copper systems.

Geological background

The study area is dominated by the Early Cretaceous Cerro del Pingo Plutonic Complex (Fig. 1). This is a large calc-alkaline intrusive complex that includes a wide range of medium- to coarse-grained plutonic rocks ranging in composition between gabbro and granite (Ulriksen 1979; Boric et al. 1990). Biotite (and locally hornblende)-bearing monzogranite and granodiorite are by far the most abundant rock types. In general, early diorite (ca. 130 Ma) is crosscut by granodiorite and tonalite intrusions (129.2±1.5 to 107.4±0.5 Ma; Berg et al. 1983; Dallmeyer et al. 1996; Gelcich et al. 2005). Geochemical studies indicate that these magmatic rocks have a geochemical signature compatible with a mantle derivation with negligible crustal contamination (Berg et al. 1983; Marschik et al. 2003).

The major geologic structure in the area is the Atacama Fault System, a NS-trending, steeply dipping trans-crustal structure active since early Mesozoic times (Cembrano et al. 2005). Most magnetite–apatite and IOCG deposits of northern Chile occur in its vicinity usually related to second order faults (Sillitoe 2003; Cembrano et al. 2005).

Deposit geology

The Tropezón Cu–Mo–(Au) deposit is currently mined by Minera Cenizas Ltda. Total resources are estimated at about 1 Mt of hypogene ore and 0.5 Mt of supergene ore (http://www.cenizas.cl). Grades of the hypogene ore are ~1% Cu

in the upper zone and ~0.13% Mo in the lower parts of the deposit. Molybdenum in the upper zone is below 0.04% and Cu in the lower zone is below 0.05%. The mineralization is located in the central part of the Cerro del Pingo Plutonic Complex and is hosted by a small intrusion (Tropezón Stock; about 2 km^2) of medium-grained clinoamphibole- or pyroxene-bearing quartz diorite to tonalite. Laser ablation multicollector ICP–MS U–Pb zircon dating of this unit has yielded a weighted average $^{206}Pb/^{238}U$ age of 110.0±2.1 Ma (n=33; MSWD=1.17) (Fig. 2), indicating that it was intruded during the waning stages of the Early Cretaceous magmatic event. This intrusion crosscuts the dominant granodiorite and monzogranite of the Cerro del Pingo Plutonic Complex (Fig. 1).

The Cerro del Pingo Plutonic Complex and the andesitic host rocks show a widespread and irregular propylitic (chlorite–sericite–epidote–calcite) alteration. This alteration zone, of unknown extent, is mainly controlled by NE–SW and ENE–WSW to ESE–WNW-trending faults (Fig. 1). The Tropezón Stock shows a more pervasive and zoned potassic–(calcic) alteration, which comprises an external biotite zone that grades inward to K-feldspar–biotite±tourmaline and K-feldspar–actinolite±tourmaline zones. The hydrothermally altered rocks contain between 1 and 3 vol.% magnetite. The plutonic host rocks adjacent to the Tropezón Stock show only sparse potassic–(calcic) alteration.

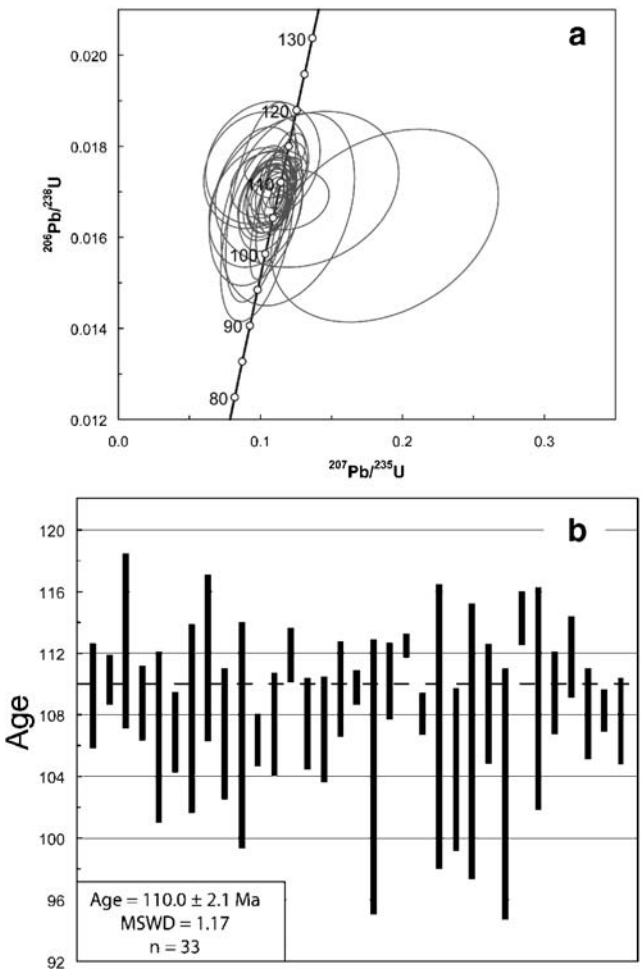

Fig. 2 **a** $^{206}Pb/^{238}U$ vs. $^{207}Pb/^{235}U$ concordia plot for the Tropezón stock. **b** Plot of $^{206}Pb/^{238}U$ crystallization ages for the Tropezón stock. Zircons were separated from the rock sample, mounted in epoxy and later analyzed using LA–multicollector–ICP–MS according to the procedure described in Gehrels et al. (2008)

The most conspicuous feature of the Tropezón deposit is the presence of two sub-vertical pipe-like tourmaline breccia bodies, each 30–60 m in diameter, in which coarse-grained euhedral tourmaline with accessory quartz, magnetite, K-feldspar, molybdenite, pyrite, chalcopyrite, and traces of albite and anhydrite support and replace 2–50 cm-sized angular to sub-rounded fragments of the Tropezón Stock with potassic–(calcic) alteration (Fig. 3). Similar tourmaline breccia bodies are found elsewhere in the Andes related to porphyry copper (e.g., Skewes et al. 2003) and tin deposits (Lehmann et al. 2000). Downwards, at about 100 m below the surface, the breccia ends into a large dome-shaped zone of Ca–Fe–K alteration. Here, the quartz diorite is replaced by a pervasive alteration assemblage that includes early massive actinolite $\left(Fe/Fe+Mg=0.23;\ Al^{VI}=0.1-0.3\right)$ with fine-grained magnetite and younger K-feldspar, epidote (ps_{30-33}), quartz, magnetite, pyrite, and tourmaline, overprinted by late chlorite, calcite, quartz, epidote, and pyrite (Fig. 3). Locally, this late assemblage includes significant amounts of hematite. In other deposits of the Coastal Cordillera of Chile, such as Candelaria and Carola, the early iron oxide phase is hematite (e.g., Marschik and Fontbote 2001), usually replaced by magnetite (mushketovite). In Tropezón, the amount of mushketovite is accessory and most of the magnetite occurs in anhedral to subhedral grains. Hematite occurs in late veins or replacing earlier magnetite.

Anhydrite, bassanite, and scapolite occur as irregularly distributed patches. The innermost alteration zone comprises massive quartz replacing the Ca–Fe–K hydrothermal assemblage. Crosscutting relationships show that the tourmaline breccia postdated the potassic–(calcic) alteration zone, but predated the more localized Ca–Fe–K and quartz alteration zones.

The bulk of the Cu–Mo–(Au) mineralization at Tropezón is related to the Ca–Fe–K alteration zone and includes chalcopyrite, molybdenite, bornite, and gold ($Au_{91}Ag_9$). Most of the mineralization is intergrown or in small veinlets within the actinolite or the K-feldspar–epidote–quartz rocks. The downward extent and shape of the orebody is unknown; however, it shows a clear zonation with an upper Cu–Au-rich shell about 50 m thick and a lower part that hosts the Mo mineralization; the contact between both zones is sub-horizontal and sharp (Fig. 4). The deposit shows major supergene alteration that can reach 100 m deep along minor faults.

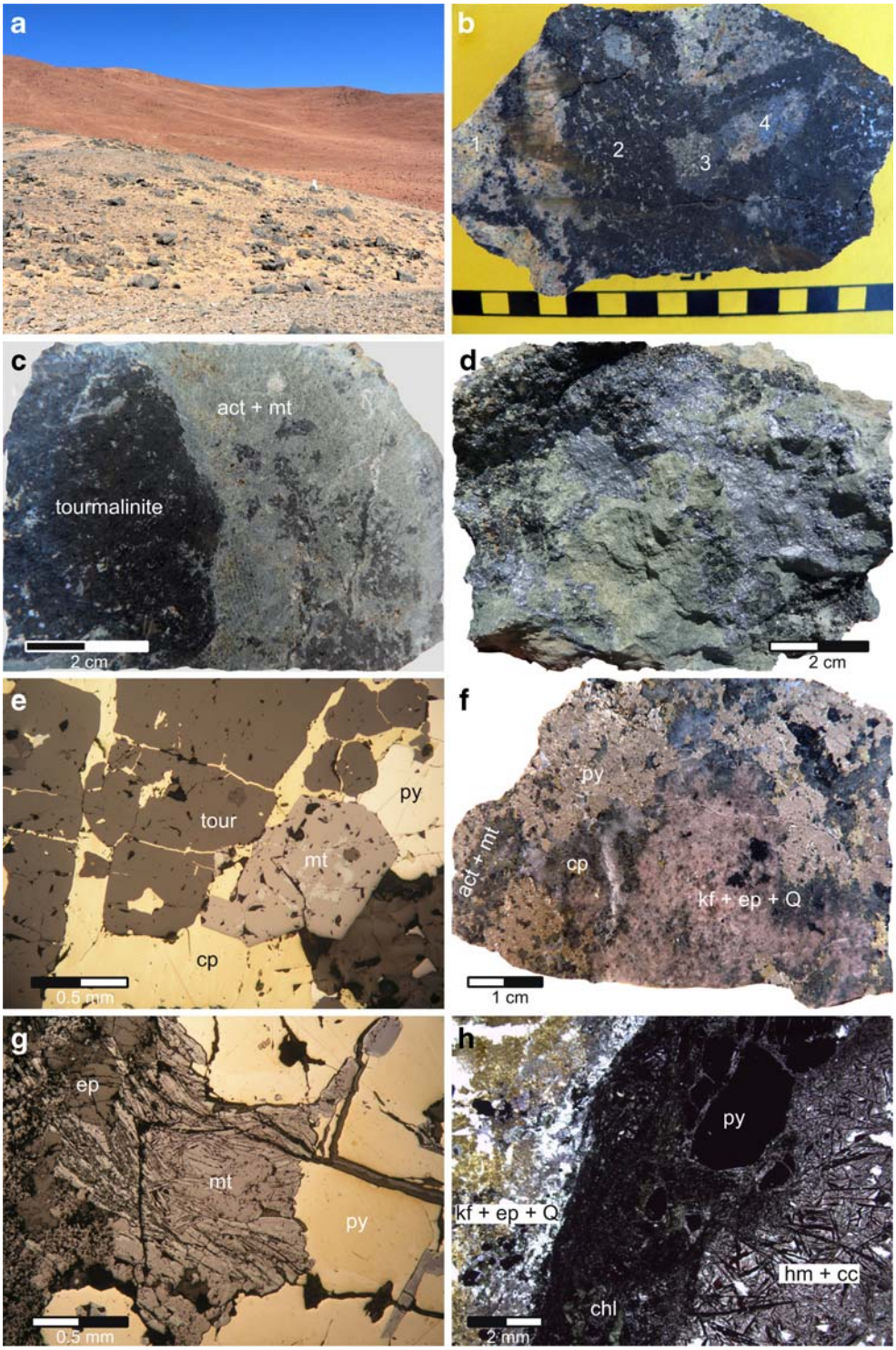

Fig. 3 Photographs of selected outcrops, rocks, and hydrothermal mineral assemblages. **a** Sub-horizontal contact between the regional granodiorite–tonalite of the Cerro del Pingo Plutonic Complex and the intruding quartz diorite. The landmark in the middle of the photo is 80 cm high. **b** Hand sample of the Tropezón ore showing the superposition of hydrothermal assemblages. *1* Breccia with fragments of quartz diorite with pervasive alteration to K-feldspar +(actinolite+magnetite) supported by tourmaline with quartz, magnetite, and molybdenite. *2* Massive actinolite intergrown with magnetite. *3* Ore-bearing assemblage including epidote, quartz, K-feldspar, magnetite, pyrite, and chalcopyrite. *4* Late assemblage of pyrite, calcite, chlorite, and quartz. Unit in the *scale bar* is 1 cm. **c** Tourmalinite from the breccia pipe replaced by actinolite with fine-grained magnetite, hosting some remnants of tourmaline. **d** Actinolite-rich alteration with abundant molybdenite from the lower part of the ore body. **e** Tourmaline (*tour*) and magnetite (*mt*) replaced and cemented by younger pyrite (*py*) and chalcopyrite (*cp*). The magnetite is partially replaced by younger hematite. **f** Zone of K-feldspar (*kf*), epidote (*e*), and quartz (*Q*) alteration with abundant sulfides (pyrite and chalcopyrite) replacing earlier actinolite (*act*) and magnetite (*mt*). **g** Late hematite, further replaced by magnetite (*mt*) postdating pyrite in the K-feldspar+epidote+quartz alteration. **h** Late veins of hematite (*hm*), pyrite, chlorite (*chl*), and calcite (*cc*) crosscutting earlier K-feldspar–epidote–quartz (*kf*+ *ep*+ *Q*) alteration

Near Tropezón, there are abundant prospects with iron oxide–Cu mineralization. Most of the mineralization near the breccia pipes is hosted by veins showing a mineralogical zonation with proximal quartz, actinolite, K-feldspar, magnetite and scapolite, and distal quartz-tourmaline. These veins propagate from the breccia pipes, such as in the Silvita prospect (Fig. 1). Magnetite is dominant close to the breccias while hematite is distal; pyrite and chalcopyrite are abundant in all the veins. However, mineralization within the Atacama Fault System and other areas such as at Filomena Mine (Fig. 1) occurs as small veins, breccias, and replacement bodies, always included in a halo of propylitic alteration. The ore bodies are rich in K-feldspar, sericite, chlorite, and calcite, locally with bladed texture. The metallic assemblage

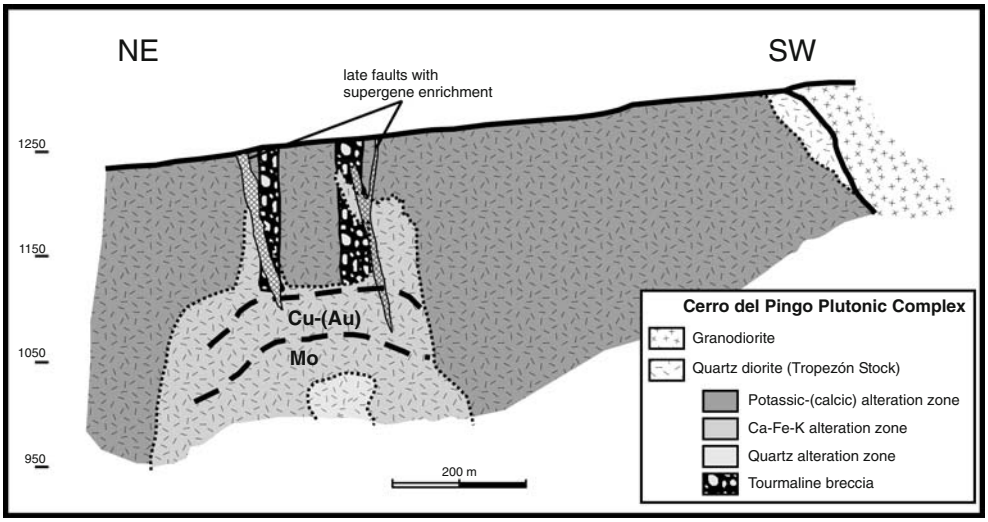

Fig. 4 Schematic cross section of the Tropezón deposit, partially based on the interpretation of Minera Cenizas. The distribution of the different hydrothermal zones is mostly inferred from the underground works and limited drillhole information

includes hematite with chalcopyrite and minor bornite. The mineralogy and the style of mineralization are similar to those of the hypogene ore of the Mantoverde, Carmen de Cobre, and other IOCG deposits of northern Chile (Sillitoe 2003; Benavides et al. 2007; Herrera et al. 2008). The size of the hematite-rich deposits near Tropezón is small, less than 1 Mt with hypogene Cu grades between 1% and 3%. At the Tropezón deposit, these veins cut the Ca–Fe–K alteration and related mineralization. They are in part responsible for the late chlorite–calcite–quartz alteration, precipitation of hematite and replacement of early magnetite by hematite.

Fluid inclusions

Fluid inclusions interpreted as primary are abundant in quartz and tourmaline. Most of them include a large (ca. 10 vol.%) halite daughter crystal and a smaller rounded isotropic crystal, probably sylvite. Other phases present include tourmaline, anhydrite, iron chlorides, hematite, and possibly chalcopyrite. Some inclusions decrepitate before homogenization, but in most cases neither the vapor bubble nor the halite crystal dissolved in the liquid phase at 500°C. A few melting temperatures of sylvite (119–280°C) and halite (294–470°C), before total homogenization by bubble disappearance at 328–490°C, indicate salinities of about 21–25 wt% KCl and 25–47 wt% NaCl. Some fluid inclusions that did not homogenize at 500°C suggest salinities higher than 70 wt% NaCl eq. Preliminary LA ICP–MS analysis shows that the fluids belong to the Na–K–Ca–Fe–Cl system. Tourmaline crystals hosted in the fluid inclusions did not change in shape and size during heating, suggesting that they are trapped phases. In the tourmaline breccia, these high-salinity fluid inclusions coexist with dominant vapor-rich inclusions having only a small rim of liquid $(1/1+v0.2)$ but no daughter or included minerals. Phase changes could not be accurately determined in these inclusions, but most did not homogenize at 500°C. Vapor-rich inclusions dominate in the tourmaline breccias, but they have not been found in the Ca–Fe–K alteration zone.

Fractures host secondary aqueous halite-saturated inclusions enriched in Fe–Mg–K–Cl that homogenize near 160–250°C; equivalent inclusions are primary in the hematite-rich veins.

Tropezón: the transition of a porphyry copper to IOCG system?

Tropezón: a magmatic–hydrothermal ore deposit?

The geology and geochemistry of the Tropezón deposit indicate that it formed during the exsolution of hydrothermal fluids from a crystallizing pluton. This model is supported by the observed relationship with a discrete intrusion, the presence of tourmaline breccia pipes, a zoned hydrothermal alteration in an intrusive unit, and relationship with the circulation of polysaline aqueous brines. Similar features are found in many magmatic–hydrothermal systems and more specifically in several porphyry copper deposits of the Andes (Sillitoe and Perelló 2005). Tropezón has also features akin to the IOCG clan, including the hydrothermal assemblage, dominated by calc-silicates, K-feldspar and magnetite (a characteristic typical of the IOCG style, Williams et al. 2005), the abundance of magnetite, the relationship with intrusive rocks of intermediate-basic composition, and the existence of a late or distal event with hematite–chalcopyrite mineralization (Fig. 5). The hydrothermal zoning in the Tropezón deposit is different to that commonly observed in porphyry copper systems (Lowell and Guilbert 1970).

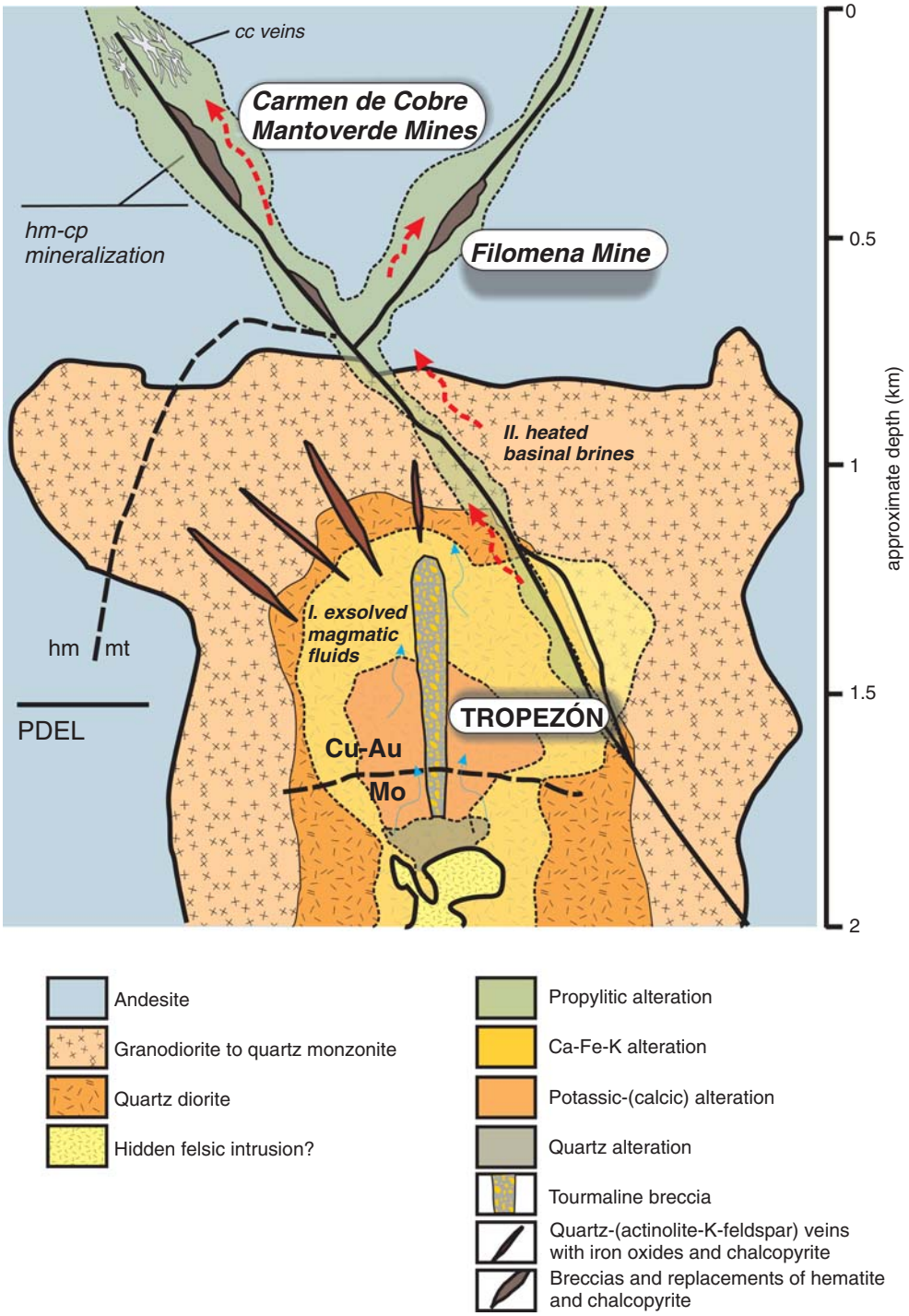

Fig. 5 Metallogenetic cartoon for the Tropezón orebody and associated IOCG deposits. Two hydrothermal events are recognized: the first one is related to the early Cretaceous magmatism leading to the formation of Tropezón (and perhaps Candelaria) deposits in rather deep environments. The second event is dominated by external fluids (basinal brines) of lower temperature leading to the formation of hematite-rich deposits similar to Mantoverde and Carmen de Cobre. Not to scale. *PDEL* present-day erosion level at Tropezón mine

Sericitic and argillic alteration zones are not present at Tropezón; instead, a dominant and more alkaline Ca–Fe–K alteration is observed.

Porphyry copper systems are characterized by the superimposition of different magmatic units that produce a complex arrangement of intrusions, hydrothermal alteration zones and different types of ore-bearing and barren hydrothermal veins (e.g., Beane and Titley 1981). The case at Tropezón is different, with pervasive hydrothermal alteration and mineralization related to a single intrusion. In porphyry systems, the ore is mostly breccia- or stockwork-related, whereas at Tropezón most of the hydrothermal assemblage is replacive, in a metasomatic cap above a presumed fluid source. Except for the tourmaline breccia pipes, there is no evidence of major fluid overpressure and hydrothermal cracking. This strongly suggests that the rock column was thick enough to prevent widespread hydrothermal rock failure. In general, the early

Cretaceous plutonism of the Coastal Cordillera intruded at lithostatic pressures between 1.5 and 3 kbar (Dallmeyer et al. 1996), in contrast with the maximum 0.5–1 kbar determined for porphyry-type deposits. This deeper emplacement is consistent with the paucity of porphyry textures in IOCG systems (Marschik et al. 2003). These arguments are consistent with fluid inclusion data, where the presence of high-temperature immiscible fluids in the tourmaline breccia suggests that it formed at fluid pressures below ca. 2.1 kbar (Driesner and Heinrich 2007). Immiscibility in the tourmaline breccia, but not in the younger replacive ore is interpreted as caused by localized fluid overpressure, rock failure, and fluid immiscibility due to the crossing of the two-phase surface. Hydrothermal replacement and ore formation took place after brecciation in a fluid regime approaching lithostatic pressures in the single fluid phase field.

The presence of these breccias is perhaps the strongest evidence of water saturation during late stages of magma crystallization with secondary boiling. The morphology and zonation of the orebody suggest that after phase separation and upward migration of vapor due to contrasting densities and wetting characteristics, the residual brine collected at the bottom of the system and was responsible for the replacement of the host quartz diorite near the base of the breccia pipe. Immiscibility between high- and low-density fluids should promote separation of Cu–Au and Mo. Fluid inclusion analyses have shown that Cu and Au are mostly partitioned into the low-density phase (Heinrich 2005), whereas Mo is concentrated in the brine (Klemm et al. 2008). If that holds true, the Mo and Cu–Au-rich zones could reflect separation between brine and a low-density fluid.

Ore precipitation seems to be related to fluid–rock interaction synchronous with cooling, with redox changes and evolution from an early and barren reduced actinolite-rich rock to a younger and more oxidized quartz–epidote–magnetite rock. Fluid inclusion and mineralogical data show that the system cooled from near magmatic temperatures to well below 350–300°C, the temperature at which sericitic alteration typically develops in porphyry-like systems. The absence of hydrothermal assemblages indicative of acid low-temperature alteration, such as in sericitic and argillic zones, strongly suggests that the fluid composition was buffered by the host rock, i.e., fluid/rock ratios were rather low, in marked contrast with those of porphyry-like hydrothermal systems. A relatively greater depth of formation and/or a dry sub-aerial environment, as was predominant in the area since the late Triassic (Clarke 2006), probably inhibited the influx of cool meteoric fluids and the development of sericitic or argillic alteration. Redox and pH conditions buffered by a biotite–K-feldspar–magnetite assemblage favored the stability of a mineral assemblage typical of neutral or alkaline environments.

The relatively low proportion of sulfides, the abundance of magnetite, the presence of anhydrite in the hydrothermal assemblage, and the fluid inclusion data suggest that the fluids had a high $SO_4^{=}/H_2S$ ratio, a feature likely inherited from the melt. This seems to be a feature typical of many porphyry copper systems, such as El Teniente, Chile (Klemm et al. 2007). The dominance of oxidized sulfur seems to be also a key characteristic of IOCG systems (Chiaradia et al. 2006), probably inhibiting the precipitation of sulfides and favoring that of magnetite, even at intermediate temperatures.

Despite not being clearly outlined due to the pervasive hydrothermal alteration and the current level of exposure, a few pieces of evidence suggest that the core of the hydrothermal system is located above a hidden intrusion more acidic in composition than the host rock. Cathodoluminescence studies of the hydrothermal quartz from the quartz zone revealed areas with mosaic textures that likely correspond to inherited quartz phenocrysts. The high Mo grades are also consistent with a derivation from more evolved felsic melts. The presence of Mo in porphyry systems is due to the contamination of melts by lower crustal rocks in areas of thickened crust (Stein and Hannah 1985; Klemm et al. 2008). Strong enrichment of Mo is typical of acid systems more evolved than copper porphyry systems (White et al. 1981) and Mo-rich skarns are associated with granitic rocks having on average 73% to 76% SiO_2 (Meinert 1983).

Relationships with other nearby IOCG deposits

The distal and/or late hematite-rich mineralization in the Tropezón area is structurally and mineralogically similar to that of the Mantoverde deposit. Fluid inclusion studies in Mantoverde showed that the orebody was associated with the circulation of boiling connate brines at temperatures of ca. 218 to 250°C (Benavides et al. 2007). In fact, the late Na–Fe–K–Cl aqueous fluids found in Tropezón could represent the connate brines reported by Benavides et al. (2007) or Chiaradia et al. (2006) that intruded the magmatic–hydrothermal system during its waning stages, in a scheme similar to that observed in porphyry copper systems for meteoric waters. Furthermore, at Mantoverde (Benavides et al. 2007), Carmen de Cobre (Herrera, pers. comm., 2007) and several other hematite-rich deposits of the Andes, the deep extensions of the orebody include a magnetite-rich mineralization almost completely modified to hematite by late hydrothermal circulation. Basinal fluids derived from the contemporaneous Chañarcillo Group or equivalent sediments, deposited in a shallow marine back-arc basin environment (Coira et al. 1982), were presumably incorporated into hydrothermal cells controlled by the Atacama Fault System.

Conclusions

The Tropezón deposit is an IOCG deposit that shows a direct genetic relationship with an intrusion of intermediate composition and shares features of both porphyry copper and IOCG systems. The hosting quartz diorite with pervasive Cu–(Au) and Mo mineralization is mineralogically similar to some porphyry systems of the Andes. However, the evolution of the magmatic–hydrothermal system looks significantly simpler than that observed in porphyry copper deposits. At Tropezón, the hydrothermal activity and mineralization are related to a single stock emplaced at greater depth than porphyry intrusions. The Tropezón Stock seems to represent the deep magmatic–hydrothermal core zone of a much larger IOCG system, probably similar to others found in northern Chile.

The mineralization formed as a consequence of magmatic exsolution of a single pulse of alkaline Fe- and Ca-rich fluids. Early exsolved fluids formed a large zone of K–(Ca) alteration followed by the formation of a tourmaline breccia pipe, interpreted as the product of instantaneous and explosive release of magmatic fluids. The progressive reaction of these fluids with the host rocks led to Ca–Fe–K alteration and formation of a zoned orebody. This system was later overprinted by the circulation of late low-temperature basinal brines where hematite became stable.

The system is perhaps similar and broadly contemporaneous to that described by Marschik and Fontbote (2001) at Candelaria, some 220 km south, and dated at 114–117 Ma (Mathur et al. 2002; Marschik and Sollner 2006). The hydrothermal alteration is also similar, but at Candelaria many of the early magmatic–hydrothermal features are masked by the later complex hydrothermal evolution. Candelaria lacks significant Mo grades and the tourmaline breccia pipes, key features of the Tropezón deposit.

The model presented here also shares features with the model proposed by Skirrow et al. (2007) for the Olympic Dam district, with the presence of an early alteration event with K-feldspar, magnetite and calc-silicates caused by the circulation of hot (>450°C) hypersaline brines and a later influx of cooler fluids (200–300°C) that produced the hematite-rich alteration.

Acknowledgments This study has been supported by the project CICYT–FEDER CGL2006-0378 of the Spanish Government and by internal funds of the IGME. It would not have been possible without the collaboration of Minera Cenizas Ltda, especially Manuel Erazo and Walter Gil that granted access to the mine site and helped with the information they could provide. U–Pb dating was performed at the Arizona LaserChron Center of the University of Arizona. Thanks are extended to Mario Arrieta, Verónica Herrera, Edgar Arocutipa, Mario Rojo, Haroldo Lledó, Eduardo Campos, and Martin Reich for helping us with different aspects of this project. Nick Badham, Marco Zentilli, and Chris Heinrich are also thanked for their help in the interpretation of the deposit, as well as Murray Hitzman for a previous review of the manuscript. Finally, it has benefited from the thoughtful comments of Lluis Fontboté, an anonymous referee, and the editor Bernd Lehmann.

References

Badham JPN (1978) Magnetite–apatite–amphibole–uranium and silver–arsenide mineralizations in Lower Proterozoic igneous rocks, East Arm, Great Slave Lake, Canada. Econ Geol 73:1474–1491

Barton MD, Johnson DA (1996) Evaporitic source model for igneous-related Fe oxide–(REE–Cu–Au–U) mineralization. Geology 24:259–262

Beane RE, Titley SR (1981) Porphyry copper deposits. Part II: hydrothermal alteration and mineralization. In: Skinner BJ (ed) Economic Geology 75th Anniversary Volume. Society of Economic Geologists, pp 235–269

Benavides J, Kyser TK, Clark AH, Oates CJ, Zamora R, Tarnovschi R, Castillo B (2007) The Mantoverde iron oxide–copper–gold district, III region, Chile: the role of regionally derived, nonmagmatic fluids in chalcopyrite mineralization. Econ Geol 102:415–440

Berg K, Breitkreuz C, Damm KW, Pichowiak S, Zeil W (1983) The North-Chilean Coast Range—an example for the development of an active continental margin. Geol Rundsch 72:715–731

Boric R, Diaz F, Maksaev V (1990) Geologia y yacimientos metaliferos de la region de Antofagasta. Bol Serv Nac Geol Min 40:1–246

Cembrano J, Gonzalez G, Arancibia G, Ahumada I, Olivares V, Herrera V (2005) Fault zone development and strain partitioning in an extensional strike–slip duplex: a case study from the Mesozoic Atacama fault system, Northern Chile. Tectonophysics 400:105–125

Chiaradia M, Banks D, Cliff R, Marschik R, de Haller A (2006) Origin of fluids in iron oxide–copper–gold deposits: constraints from $\delta^{37}Cl$, $^{87}S/^{86}Sr_i$ and Cl/Br. Miner Deposita 41:565–573

Clarke JDA (2006) Antiquity of aridity in the Chilean Atacama Desert. Geomorphology 73:101–114

Coira B, Davidson J, Mpodozis C, Ramos V (1982) Tectonic and magmatic evolution of the Andes of northern Argentina and Chile. Earth-Sci Rev 18:303–332

Dallmeyer RD, Brown M, Grocott J, Taylor GK, Treloar PJ (1996) Mesozoic magmatic and tectonic events within the Andean Plate Boundary Zone, 26°–27°30′S, North Chile: constraints from $^{40}Ar/^{39}Ar$ mineral ages. J Geol Soc 104:19–40

Driesner T, Heinrich CA (2007) The system H_2O–NaCl. Part I. Correlation formulae for phase relations in temperature–pressure–composition space from 0 to 1000°C, 0 to 5000 bar and 0 to 1 XNaCl. Geochim Cosmochim Acta 71:4880–4901

Gehrels GE, Valencia VA, Ruiz J (2008) Enhanced precision, accuracy, efficiency, and spatial resolution of U–Pb ages by laser ablation–multicollector–inductively coupled–mass spectrometry. Geochem Geophys Geosyst 9. doi:10.1029/2007GC001805

Gelcich S, Davis DW, Spooner ETC (2005) Testing the apatite–magnetite geochronometer: U–Pb and $^{40}Ar/^{39}Ar$ geochronology of plutonic rocks, massive magnetite–apatite tabular bodies and IOCG mineralization in Northern Chile. Geochim Cosmochim Acta 69:3367–3384

Grocott J, Taylor GK (2002) Magmatic arc fault systems, deformation partitioning and emplacement of granitic complexes in the Coastal Cordillera, north Chilean Andes (25°30′S to 27°00′S). J Geol Soc 159:425–442

Heinrich C (2005) The physical and chemical evolution of low-salinity magmatic fluids at the porphyry to epithermal transition: a thermodynamic study. Miner Deposita 39:864–889

Herrera V, Garmendia P, Pizarro R (2008) Proyecto Diego de Almagro: Geología y mineralización tipo IOCG, región de Atacama, Norte de Chile. Abstr XIII Congreso Latinoamericano de Geología. Lima, S03

Hitzman MW, Oreskes N, Einaudi MT (1992) Geological characteristics and tectonic setting of Proterozoic iron-oxide (Cu–U–Au–REE) deposits. Precambrian Res 58:241–287

Klemm LM, Pettke T, Heinrich CA, Campos E (2007) Hydrothermal evolution of the El Teniente deposit (Chile): porphyry Cu–Mo

ore deposition from low salinity magmatic fluids. Econ Geol 102:1021–1045

Klemm LM, Pettke T, Heinrich CA (2008) Fluid and source magma evolution of the Questa porphyry Mo deposit, New Mexico, USA. Miner Deposita 43:533–552

Lehmann B, Dietrich A, Heinhorst J, Métrich N, Mosbah M, Palacios C, Schneider H, Wallianos A, Webster J, Winkelmann L (2000) Boron in the Bolivian tin belt. Miner Deposita 35: 223–232

Lowell JD, Guilbert JM (1970) Lateral and vertical alteration–mineralization in porphyry deposits. Econ Geol 65:378–404

Mark G, Foster DRW, Pollard PJ, Williams PJ, Tolman J, Darvall M, Blake KL (2004) Stable isotope evidence for magmatic fluid input during large scale Na–Ca alteration in the Conclurry Fe oxide Cu–Au district, NW Queensland, Australia. Terra Nova 16:54–61

Marschik R, Fontbote L (2001) The Candelaria–Punta del Cobre iron oxide Cu–Au(–Zn–Ag) deposits, Chile. Econ Geol 96:1799–1828

Marschik R, Sollner F (2006) Early Cretaceous U–Pb zircon ages for the Copiapo plutonic complex and implications for the IOCG mineralization at Candelaria, Atacama Region, Chile. Miner Deposita 41:785–801

Marschik R, Fontignie D, Chiaradia M, Voldet P (2003) Geochemical and Sr–Nd–Pb–O isotope composition of granitoids of the Early Cretaceous Copiapó Plutonic Complex (27°30′S), Chile. J South Am Earth Sci 16:281–398

Mathur R, Marschik R, Ruiz J, Munizaga F, Leveille RA, Martin W (2002) Age of mineralization of the Candelaria Fe Oxide Cu-Au deposit and the origin of the Chilean Iron belt, based on Re-OS isotopes. Econ Geol 97:59–71

Meinert LD (1983) Variability of skarn deposits: guides to exploration In: Boardman SJ (ed) Revolution in the earth sciences—advances in the past half century. Kendall Hunt, Dubuque, pp 301–316

Naranjo JA, Puig A (1984) Hojas Taltal y Chañaral, regiones de Antofagasta y Atacama. Servicio Nacional de Geología y Minería, Santiago

Pollard PJ (2000) Evidence for magmatic fluid and metal source for Fe–oxide Cu–Au mineralization. In: Porter TM (ed) Hydrothermal Iron Oxide Copper–Gold & Related Deposits: A Global Perspective. Australian Mineral Foundation, Adelaide, pp 27–41

Sillitoe RH (2003) Iron oxide–copper–gold deposits: an Andean view. Miner Deposita 38:787–812

Sillitoe RH, Perelló J (2005) Andean copper province: tectonomagmatic settings, deposit types, metallogeny, exploration, and discovery. In: Hedenquist JW, Thompson JFH, Goldfarb RJ, Richards JP (eds) Economic geology—100th anniversary volume. Society of Economic Geologists, Littleton, pp 845–890

Skewes MA, Holmgren C, Stern CR (2003) The Donoso copper-rich tourmaline bearing breccia pipe in Central Chile: petrologic, fluid inclusion and stable isotope evidence for an origin from magmatic fluids. Miner Deposita 38:2–21

Skirrow RG, Bastrakov EN, Baroncii K, Fraser GL, Creaser RA, Fanning CM, Raymond OL, Davidson GJ (2007) Timing of iron oxide Cu–Au–(U) hydrothermal activity and Nd isotope constraints on metal sources in the Gawler craton, south Australia. Econ Geol 102:1441–1470

Stein HJ, Hannah JL (1985) Movement and origin of ore fluids in Climax-type systems. Geology 13:469–474

Ulriksen CE (1979) Regional geology, geochronology and metallogeny of the Coastal Cordillera of Chile between 25°30′ and 26° South. Ms Thesis, Dalhousie University, pp 221

White WH, Bookstrom A, Kamilli RJ, Ganster MW, Smith RP, Ranta DE, Steininger RC (1981) Character and origin of Climax-type molybdenum deposits. In: Skinner BJ (ed) Economic Geology—100th Anniversary Volume. Society of Economic Geologists, Littleton, pp 270–316

Williams P, Barton MD, Johnson DA, Fontboté L, Ad H, Mark G, Oliver NHS, Marschik R (2005) Iron oxide copper–gold deposits: geology, space–time distribution, and possible modes of origin. In: Hedenquist JW, Thompson JFH, Goldfarb RJ, Richards JP (eds) Economic Geology—100th Anniversary Volume. Society of Economic Geologists, Littleton, pp 371–406